Optical and Quantum Electronics (2023) 55:929
https://doi.org/10.1007/s11082-023-05197-7

Impact of optical device parameters on the performance characteristics of temperature dependent quantum cascade lasers

Abdulkarem H. M. Almawgani[1] · B. Ramasubba Reddy[2] · Turki Alsuwian[1] · P. Ashok[3] · C. R. Rathish[4] · M. Ganesh Madhan[5]

Received: 11 May 2023 / Accepted: 15 July 2023 / Published online: 8 August 2023

Abstract
Temperature dependent Quantum Cascade Lasers are known for their advantages when compared to conventional lasers. In this work, we will focus on their temperature dependent capabilities. This research work reports the impact of optical device parameters on the transient and steady state dynamics of the device. Also, analysis on the analog modulation characteristics on the device is carried out in detail. The parameters namely terminal voltage (V), spontaneous emission factor (β), number of stages (M) and mirror reflectivity (R) are varied under different cold finger temperature conditions to evaluate their effect on the device characteristics. Bandwidth, maximum modulation depth, and corresponding frequency are investigated while the device is being powered by a haversine input current. From the analysis, it is found that as the cold finger temperature is increased, the lasing action is delayed leading to increase in threshold current irrespective of variation in any device parameter. Also, maximum Modulation Depth (MD) of 18% is obtained when T = 45 K and driven with 0.65 A current. When the injected current is 1.05 A at T = 15 K, maximum bandwidth of 27 GHz is produced. The minimum frequency to produce maximum MD increases with increase in current and cold finger temperatures.

Keywords Optical device · Quantum cascade lasers (QCLs) · Cold finger temperature · Modulation depth (MD) · Terminal voltage · Cold finger temperature · Bandwidth

1 Introduction

QCLs are compact but powerful sources with their mid-infrared wavelength operations. At higher temperature operation, the escape of electrons impacts the optical injection efficiency, threshold current and output power of a QCL (Page et al. 1999; Kruck et al. 2000). Other parameters that affect the operation of a mid-infrared laser include the non-radiative scattering times and the electroluminescence spectrum. In reality, the device's working temperature is constrained by these characteristics. Experimental results suggest room temperature operation of a mid-infrared QCL (Jirauschek and Tzenov 2017). Also,

Extended author information available on the last page of the article

in the absence of magnetic field, the device can provide stable operation up to 200 K (Page et al. 2001). A detailed investigation on the impact of device parameters in a 9 μm QCL, short optical pulse generation by gain switching are presented in Fathololoumi et al. (2012), Ashok and Ganesh Madhan (2019a). The application of QCL in free space optical communication is explored in detail in Ashok and Ganesh Madhan (2020a), Ashok and Ganesh Madhan (2019b), Arafin et al. (2012), Ashok and Ganesh Madhan (2020b). The intrinsic impedance characteristics of QCL are well reported in Ashok and Ganesh Madhan (2021a). Other related works pertaining to this study are available in Gopinath et al. (2021), Ashok and Ganesh Madhan (2021b), Winge and Wacker (2014). The model reported in Murali Krishna et al. (2020), Hu et al. (2015) accounts for temperature and voltage dependence of all parameters in the reduced rate equation. The device under consideration in the research has a threshold current of 0.44 A at 15 K, 0.49 A at 35 K, and 0.54 A at 45 K (Murali Krishna et al. 2020). Room temperature operation of QCLs is possible now. One such, directly modulated QCL operating at 9.15 μm is used in free space optical transmission with data rates up to 5.1Gbps at a bit error rate of $6.25*10^{-2}$ (Ashok et al. 2020). The QCL employed a frequency domain equalizer to combat the effects of pulse spreading. The possibility of using QCL with an external cavity for tuneability in the terahertz domain is well documented (Krishna et al. 2020; Kim et al. Jan. 2023). QCLs and QCDs are promising candidates for free space optics communication system where high bandwidth, low energy consumption, large scale deployment are the requirements. A FSO link employing directly modulated QCL operating at 9.6 μm, under different data rates and at different temperatures is studied (Kamruzzaman et al. 2022). These findings point to a substantial advancement in the direction of the envisioned fully-connected mid-IR FSO system driven by silicon quantum cascade devices. High-quality beam patterns and variable power output may be achieved using the device's continuous, wideband tweaking. It is widely established that dislocation filtering allowed for the growth of an InP-based long wavelength quantum cascade laser on a Silicon substrate (Agnew, et al. 2015; Joharifar, et al. 2023). The laser operating above 373 K, emits a peak power of 4 W at 10.8 μm. The far field pattern of the beam shape is single lobed, exhibiting fundamental transverse mode operation. High power QCLs with four Aluminium quantum wells to suppress escape of electrons and scattering effects operate in the frequency range 3.8–4.05 THz (Han, et al. 2023; Hu et al. 2015; Slivken and Razeghi 2022; Li, et al. 2022; Bai and Citrin 2008; Alqahtani et al. 2023). The device exhibited superior performance at lower temperatures with peak power output. The effect of the device parameters on the steady state and transient characteristics and the analog modulation characteristics of the device have not been explored till date. Hence, a detailed analysis is carried out to ascertain the applications of the device in Radio-over-Fiber (RoF) areas. It helps in ascertaining the bandwidth and modulation depth when the device is used for real time applications. To examine the impact of device settings on device characteristics, we numerically solve the reduced rate equations using MATLAB's ODE solver.

This research work is organized as follows. Section 2 explains the characteristics of temperature dependent QCLs analyzed using reduced rate equation model. Section 3 accounts for the analysis of the effect of various device parameters on the device characteristics. Section 4 explores the analog modulation characteristics of the device and summarizes the findings.

2 Characteristics of temperature dependent QCLs

Temperature dependent QCLs operating at 2.59 THz up to 50 K are made of GaAs/AlGaAs. Cryogenic operation is achieved by mounting the QCL and waveguide configuration atop a copper cold finger, as shown in Fig. 1. The waveguides have a negligible influence on the metal cold finger's effective temperature.

The parameters that are considered in the numerical analysis are number of stages (M), mirror reflectivity (R), terminal voltage (V) and spontaneous emission factor (β). They play a greater role in impacting the steady state characteristics of the device. The reduced rate equations of QCL are given below (Murali Krishna et al. 2020):

$$\frac{dS(t)}{dt} = \frac{-S(t)}{\tau_p} + \frac{\beta_{sp}}{\tau_{sp}(T,V)}N_3(t) + MG(T,V)\frac{\left(N_3(t)-N_2(t)\right)}{1+\epsilon S(t)}S(t) \tag{1}$$

$$\frac{dN_3(t)}{dt} = -G(T,V)\frac{\left(N_3(t)-N_2(t)\right)}{1+\epsilon S(t)}S(t) - \frac{1}{\tau_3(T,V)}N_3(t) + \frac{\eta_3(T,V)}{q}I(t) \tag{2}$$

$$\frac{dN_2(t)}{dt} = G(T,V)\frac{\left(N_3(t)-N_2(t)\right)}{1+\epsilon S(t)}S(t) + \frac{1}{\tau_{32}(T,V)}N_3(t) + \frac{\eta_2(T,V)}{q}I(t) - \frac{1}{\tau_{21}(T,V)}N_2(t) \tag{3}$$

$$\frac{dT(t)}{dt} = \frac{1}{mc_p}\left(I(t)V(T(t),I(t)) - \frac{(T(t)-T_0)}{R_{th}}\right) \tag{4}$$

where I(t) is the injected current, S(t) is the photon number, $N_3(t)$ and $N_2(t)$ are the carrier numbers in upper and lower lasing levels respectively. The temperature of the device's active zone is modelled by Eq. (4). The rate equations as in Eq. (1–4) describe the dynamics of carrier populations and photon generation within the device, thereby providing valuable insights into its performance and characteristics. Carrier dynamics, threshold current, output characteristics, gain and loss, modulation response are some of the characteristics that can be derived from the rate equations. Since the device is temperature dependent, several parameters in the rate equations are presented as functions of both voltage and temperature (Murali Krishna et al. 2020). The rate equations are solved numerically to determine the steady state characteristics of the device under voltage dependent case (V = 2.80 V). Figure 2 shows that for 15 K, 35 K, and 45 K, the threshold current of the device is 0.4 A, 0.44 A, and 0.49 A, respectively. The steady-state features findings are consistent with Agnew et al. (2015), proving the validity of our simulation method. In the next section, the impact of the device parameters namely terminal voltage (V), spontaneous emission factor

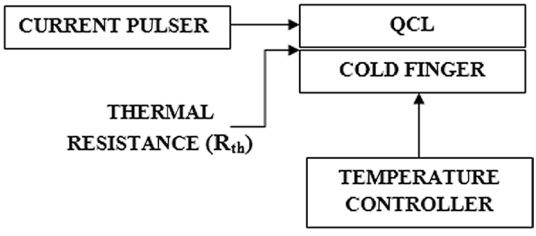

Fig. 1 QCL with temperature controller arrangement

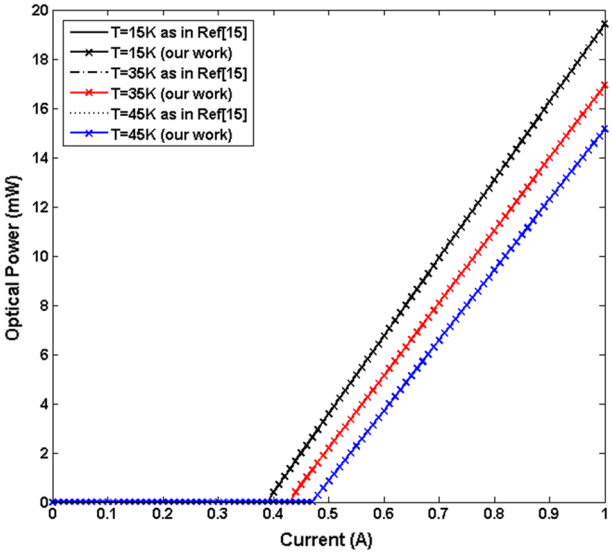

Fig. 2 Voltage dependent steady state (P–I) characteristics of QCL (V = 2.80 V)

(β), number of stages (M) and mirror reflectivity (R) under different cold finger temperature conditions on the device characteristics is evaluated.

2.1 Impact of number of stages (M)

The number of stages (M) is determined by the manufacturing method and corresponds to the number of cascaded quantum wells utilised to create the laser emission. Increasing the number of stages in a QCL can lead to several benefits, including higher output power, improved efficiency, and broader tuning ranges. However, it can even lead to higher operating temperatures, which can reduce the lifetime of the laser. Two parts make up a stage in QCL: the injector and the active. Each stage is replicated a fixed number of times to produce cascading effect of electrons. The standard values taken by M are 48, 60, 72, 90 (Fathololoumi et al. 2012; Murali Krishna et al. 2020). The analysis is performed by changing M and T while all other parameters are held constant. Figure 3 displays the obtained outcomes. Figure 3a shows that the threshold current and the time required to reach lasing both rise with increasing cold finger temperature for M = 90. For a given temperature 15 K, as M is varied, the optical power also increases. There is no variation in threshold current as in Fig. 3b. Larger the value of M, larger is the optical power which is due to the cascading effect of electrons. Also, when the cold finger temperature is varied, increasing M results in drop in optical power. The optical power reduces from 10 to 6.6 mW as T is varied from 15 to 45 K for M = 90 as in Fig. 3c.

2.2 Impact of mirror reflectivity ($R_1 = R_2 = R$)

The mirror reflectivity (R) plays a crucial role in determining the performance of quantum cascade lasers (QCLs). QCLs typically use two mirrors, one on each end of the laser cavity, to confine the light within the cavity and provide feedback for laser oscillation. The reflectivity of these mirrors can significantly impact the QCL's output power, threshold current,

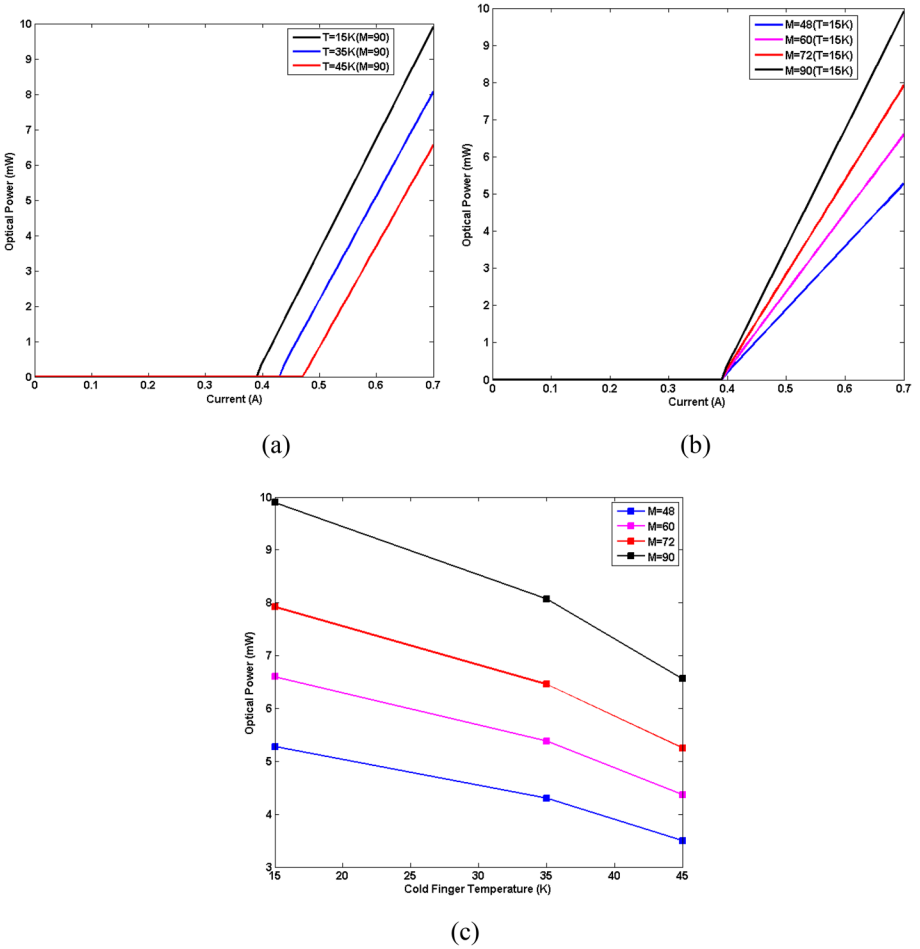

Fig. 3 **a** P–I characteristics (T = 15 K, 35 K, 45 K, M = 90) **b** P–I characteristics (M = 48, 60, 72, 90, T = 15 K) **c** cold finger temperature versus optical power characteristics

and efficiency. High reflectivity mirrors provide stronger feedback for laser oscillation, which can lead to higher output power and lower threshold current. The use of high reflectivity mirrors also allows for more efficient use of the gain medium, which can increase the overall efficiency of the laser. The use of higher reflectivity mirrors can lead to higher optical losses due to absorption and scattering within the mirrors themselves. This can limit the maximum achievable output power of the QCL and reduce the overall efficiency. It can also limit the tuning range by restricting the number of allowed cavity modes. Many applications demand high reflectivity mirrors (R = 0.998–0.99999) in lasers. They are essential components for beam steering and maximizing throughput. The variation in reflectivity of the mirrors has a direct impact on the characteristics of the device. Mirrors with reflectivity of 0.324 are used in temperature dependent QCLs because of active region constraints. The value of R considered for the study is 0.29, 0.324, 0.35, 0.38 while other parameters take standard values. The results are presented in Fig. 4. From Fig. 4a, it is observed that, for R = 0.324, as the cold finger temperature is increased, the threshold current also increases.

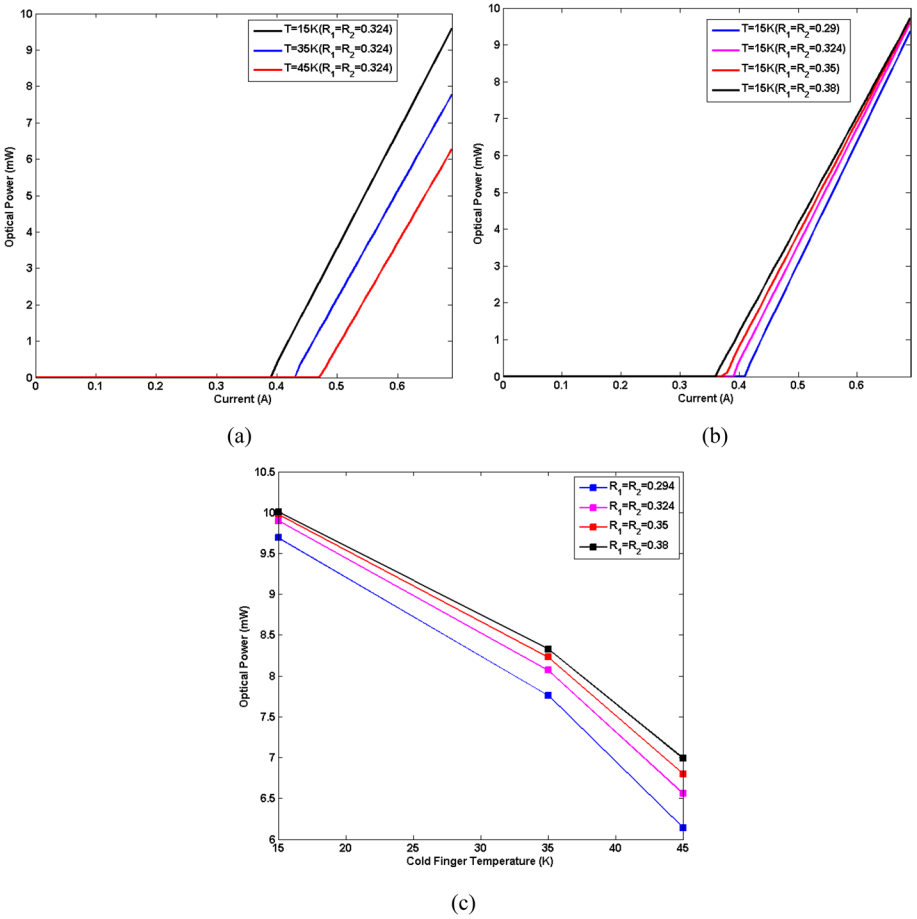

Fig. 4 **a** P–I characteristics (T = 15 K, 35 K, 45 K, R = 0.324) **b** P–I characteristics (R = 0.29, 0.324, 0.35, 0.38, T = 15 K) **c** cold finger temperature versus optical power characteristics

Since QCLs work better in cold temperatures, any increase in temperature will delay lasing thereby increasing the threshold current of the device. At a constant temperature of 15 K, when the mirror reflectivity is varied, threshold current also varies.

The mirror with the increased reflectivity is shown in Fig. 4b to have a lower threshold current and a faster lasing onset time. The similar pattern of behaviour is seen at both 35 K and 45 K finger temperatures. Any increase on cold finger temperature reduces the output power of the device. Device having mirrors with larger reflectivity produce large optical power. For R = 0.38, optical power drops from 10 to 7 mW for T = 15 K and 45 K respectively as in Fig. 4c.

2.3 Impact of terminal voltage (V)

Terminal voltage is the voltage that is applied externally to the device. The QCL operates in two modes namely voltage independent and voltage dependent mode. Under

voltage dependent mode, the externally applied terminal voltage is varied. Under voltage independent case, the terminal voltage is fitted to a function of injected current (I) and cold finger temperature (T). Mostly, QCLs are operated in voltage dependent mode. Increasing the terminal voltage (V) can increase the output power of the QCL. This is because higher voltages can lead to increased carrier injection into the active region of the QCL, resulting in higher population inversion and higher emission intensity. However, increasing the terminal voltage beyond a certain point can also lead to higher heating and reduced efficiency due to increased electron scattering and phonon emission. Higher terminal voltages can lead to lower threshold currents due to increased carrier injection into the active region of the QCL. However, there is a limit to how low the threshold current can be reduced by increasing the terminal voltage, as other factors such as material quality, doping, and waveguide design also play a role in determining the threshold current. Increasing the terminal voltage can lead to higher output power, but it can also increase the power dissipated within the laser, leading to reduced efficiency. In this study, V takes the following values 2.8 V, 3 V and 3.2 V respectively. The analysis results are presented in Fig. 5. From Fig. 5a, it is evident that increasing cold finger temperature increases the threshold current characteristics of the device. When V = 3 V, the optical power is maximum as in Fig. 5b. Lasing happens with some delay for V = 2.8 V and V = 3.2 V. As the terminal voltage is varied, the optical power decreases with increase in cold finger temperature. The optical power reduced from 10.8 to 9 mW as T is varied from 15 to 45 K. This is shown in Fig. 5c.

2.4 Impact of spontaneous emission factor (β)

The coefficient β measures how much of the overall rate of spontaneous emission was accounted for in the output. Typical values of β are in the range 10^{-3}–10^{-2}. Increasing the spontaneous emission factor can have a negative impact on the performance of temperature-dependent QCLs. This is because higher spontaneous emission reduces the efficiency of the QCL, leading to lower output power and higher threshold current. At higher temperatures, the impact of spontaneous emission becomes more significant because thermal effects lead to an increase in the number of carriers available in the active region of the QCL. As a result, the spontaneous emission factor increases, reducing the efficiency of the QCL. This effect can be particularly pronounced in high-temperature operation regimes, where the spontaneous emission factor can approach unity, resulting in significantly reduced performance. Reducing the spontaneous emission factor in QCLs can be challenging because it is often linked to the QCL's design and material properties. In the study, β takes the value $1.627*10^{-4}$. It is varied from $1.627*10^{-4}$ to $6*10^{-4}$ to study its effect on the device characteristics while all other parameters assume standard values. The results are presented in Fig. 6.

From Fig. 6a, it is seen for $\beta = 1.627*10^{-4}$, as the cold finger temperature is increased, the threshold current also increases. At a given temperature T = 15 K, there is no change in the steady characteristics of the device as evident in Fig. 6b. The optical power also reduces from 9.9 to 6.5 mW as the cold finger temperature is increased.

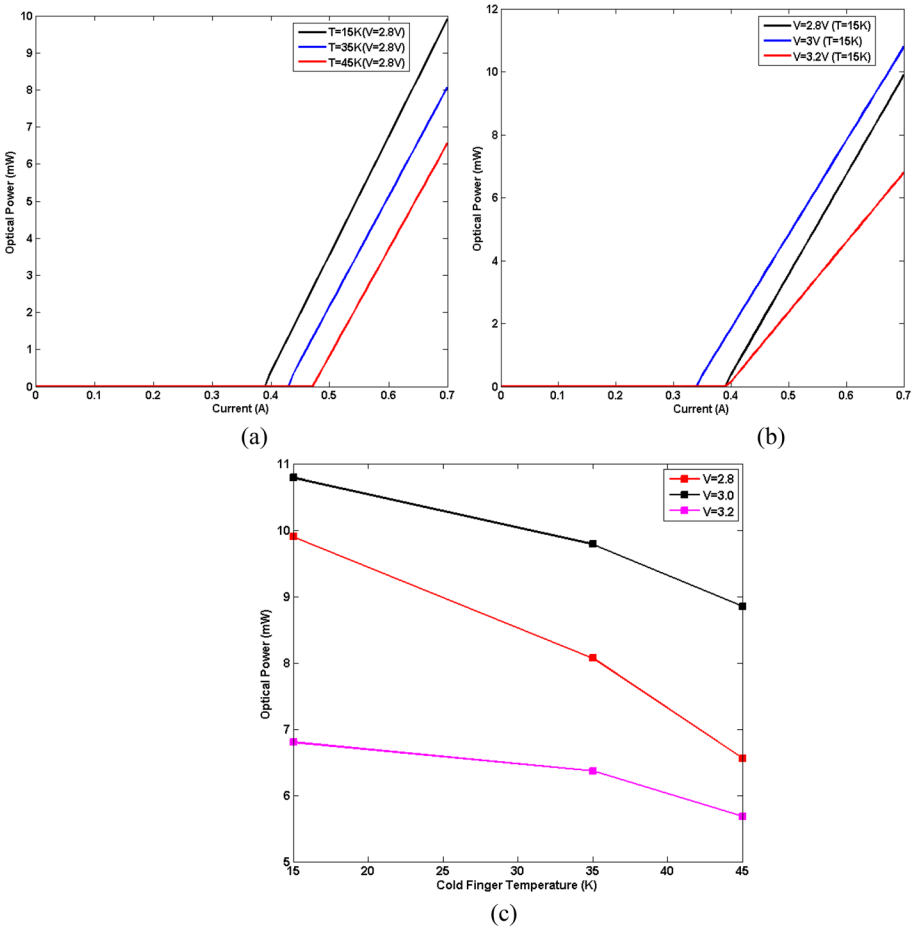

Fig. 5 **a** P–I characteristics (T = 15 K, 35 K, 45 K, V = 2.8 V) **b** P–I characteristics (V = 2.8 V, 3 V, 3.2 V, T = 15 K) **c** cold finger temperature versus optical power characteristics

3 Analog modulation characteristics

The device is driven by haversine waveform to study the frequency response. Haversine currents having peak-to-peak value of 0.65 A, 0.75 A, 0.85 A and 0.95 A are applied to the device at different cold finger temperatures with varying frequency. The modulation response is illustrated in Fig. 7.

From Fig. 7a, it is conclusive that, the device provides highest bandwidth at T = 15 K and it reduces substantially for T = 35 K and T = 45 K. The response also drops at the same rate for all the temperatures. For a given value of T, say T = 15 K, as the injected current is varied, peak overshoot is observed in the modulation characteristics. The device provides an increase in bandwidth as the amplitude of the injected current is increased enabling wide-band operation of the device. Modulation Depth (MD) is computed as in Eq. 5.

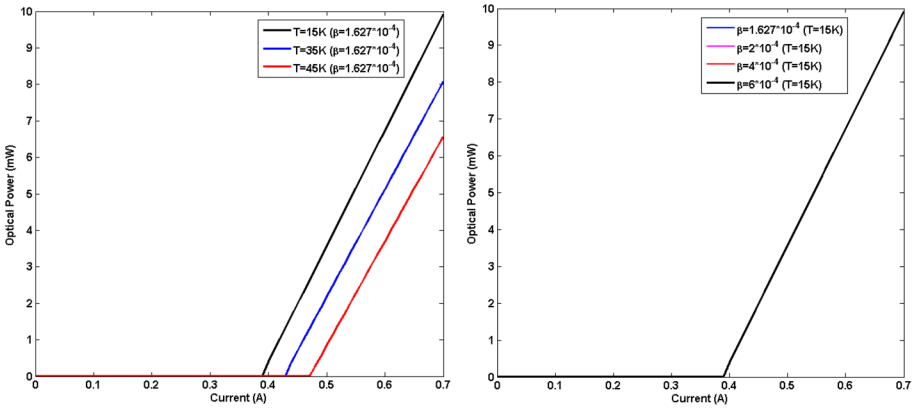

(a) (b)

Fig. 6 **a** P–I characteristics (T = 15 K, 35 K, 45 K, $\beta = 1.627*10^{-4}$) **b** P–I characteristics ($\beta = 1.627*10^{-4}$, $2*10^{-4}$, $4*10^{-4}$, $6*10^{-4}$, T = 15 K)

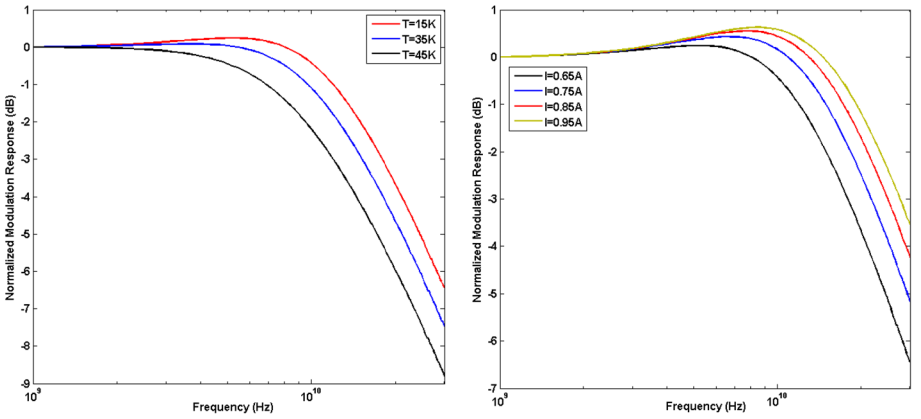

(a) (b)

Fig. 7 **a** Modulation characteristics (I = 0.65A, varying T) **b** modulation characteristics (T = 15 K, varying I)

$$MD = \frac{P_{max} - P_{th}}{P_{th}} \tag{5}$$

where P_{max} and P_{th} are the maximum and threshold optical power when the device is injected with haversine current. Additionally, the bandwidth is determined for a selection of injected currents and cold finger temperatures. The results are presented in Fig. 8. From Fig. 8a, it is found that, the device provides maximum MD at higher cold finger temperatures. When T = 45 K, maximum MD of 18% is obtained when I = 0.65 A and it drops to 10% for I = 1.05 A. Even at other temperatures, the maximum MD reduces reasonably from its peak value. However, in contrast, the frequency at which maximum MD is obtained,

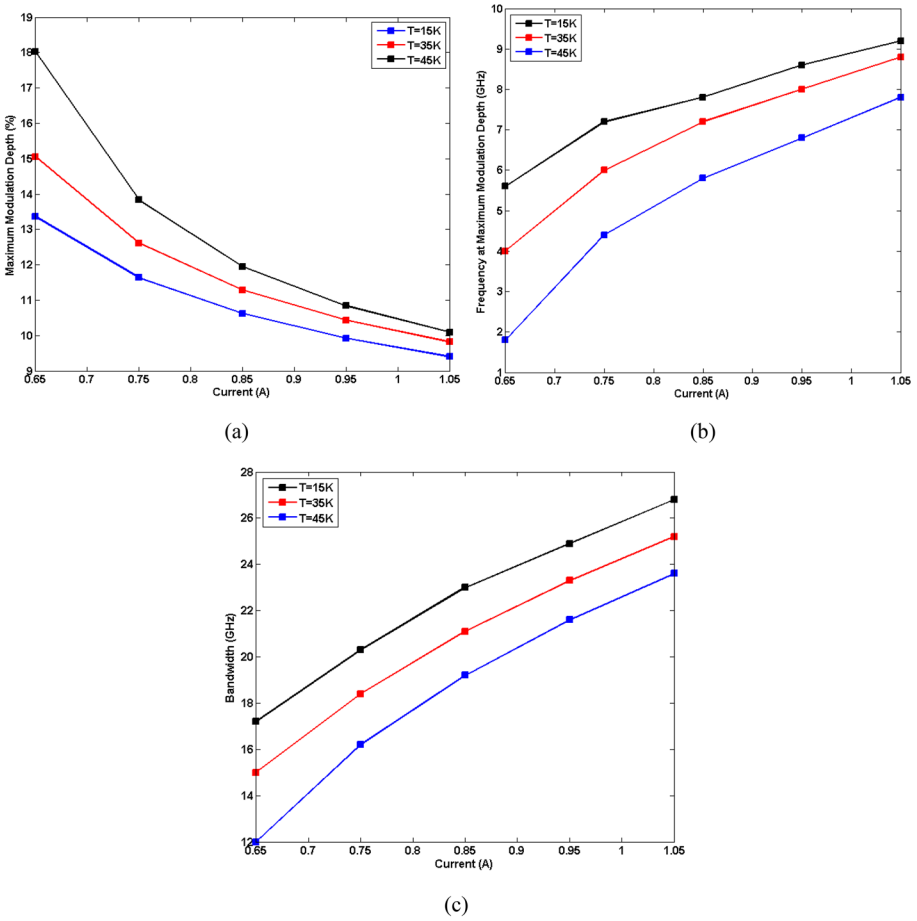

Fig. 8 Current versus **a** maximum modulation depth **b** frequency at which maximum modulation depth is obtained **c** bandwidth

increases with increasing current. At higher currents, maximum MD is obtained at higher frequencies of operation of the device as in Fig. 8b.

As shown in Fig. 8c, the device's bandwidth grows in direct proportion to the square of the current and the inverse of the cold finger temperature. Insight into the device's optimal working parameters for analogue modulation applications is provided by this study. With requirements on injected RF current, bandwidth constraints and MD, from Fig. 8, optimum value of each of the parameter can be ascertained to maximize the performance of the device. The results are summarized in Table 1.

4 Conclusion

In this paper, the effect of optical device parameters on temperature-dependent QCL features is analysed in depth, using a range of cold finger temperatures. Also, the device is driven with haversine RF current to ascertain the modulation characteristics. No

Table 1 Performance characteristics of the device under varying operating conditions

Device parameter	Measured parameter	Cold finger temperature (K)	Current (A)
No of stages (M = 90)	Peak optical power of 9.9 mW	15	0.7
Mirror reflectivity (R = 0.38)	Peak optical power of 10 mW	15	0.7
Terminal voltage (V = 3 V)	Peak optical power of 10.79 mW	15	0.7
Spontaneous emission factor (any value of β)	Peak optical power of 9.9 mW	15	0.7
Maximum MD	18%	45	0.65
Maximum bandwidth	27 GHz	15	1.05
Minimum frequency at maximum MD	5.6 GHz	15	0.65

matter what changes are made to the other parameters of the device, the research shows that the threshold current will grow as the cold finger temperature rises. Also, maximum Modulation Depth (MD) of 18% is obtained when T = 45 K and driven with 0.65 A current. When the injected current is 1.05 A at T = 15 K, maximum bandwidth of 27 GHz is produced. The minimum frequency to produce maximum MD increases with increase in current and cold finger temperatures. The goal of this research is to determine the optimal working parameters for the device. For better performance, the device should possess minimum threshold current, peak optical power, maximum MD, maximum bandwidth and the minimum frequency at which maximum MD is obtained. The amplitude and frequency of injected RF current, cold finger temperature play a major role in ascertaining the modulation characteristics of the device and its application in Radio-over-Fiber (RoF) technology.

Acknowledgements The authors certify that this material or similar material has not been and will not be submitted to or published in any other publication before. Furthermore, the authors certify that they have participated sufficiently in the work to take public responsibility for the content, including participation in the concept, design, analysis, writing, or revision of the manuscript.

Author contributions All authors contributed to the study conception and design. AHMA and RRB have done the analysis of the article. TA and AP have experienced the results with proper optimization. AP and RCR has validated the complete work and prepared the first draft of the manuscript. All authors commented on previous versions of the manuscript. All authors read and approved the final manuscript.

Funding The authors are thankful to the Deanship of Scientific Research at Najran University for funding this work under the Research Groups Funding program grant code (NU/RG/SERC/12/1).

Data and materials availability Data sharing not applicable to this article as no datasets were generated or analyzed during the current study.

Declarations

Conflict of interest The authors declares that they do not have any competing interest. The authors of this research acknowledge that they are not involved in any financial interest.

Ethics approval and consent to participate Not Applicable.

Consent for publication Not Applicable.

References

Agnew, G., et al.: Efficient prediction of terahertz quantum cascade laser dynamics from steady-state simulations. Appl. Phys. Lett. **106**(16), 161105 (2015)

Alqahtani, A.S., Kumar, U.A., Ramakrishnan, J., et al.: Investigation of hybrid spectrum slicing-wavelength division multiplexing (SS-WDM) in transparent medium for mode division multiplexing applications. Opt. Quant. Electron. **55**, 243 (2023). https://doi.org/10.1007/s11082-022-04518-6

Arafin, M.T., Islam, N., Roy, S., et al.: Performance optimization for terahertz quantum cascade laser at higher temperature using genetic algorithm. Opt. Quant. Electron. **44**, 701–715 (2012). https://doi.org/10.1007/s11082-012-9590-z

Ashok, P., Ganesh Madhan, M.: Effect of device parameters on gain switching in quantum cascade lasers. Laser Phys. Lett. **16**, 1–6 (2019a)

Ashok, P., Ganesh Madhan, M.: Performance analysis of various pulse modulation schemes for a FSO link employing gain switched quantum cascade lasers. J. Opt. Laser Technol. **111**, 358–371 (2019b)

Ashok, P., Ganesh Madhan, M.: Effect of cold finger temperature on optical pulse modulation characteristics in a 2.59 terahertz quantum cascade laser. Laser Phys. Lett. **17**, 1–7 (2020a)

Ashok, P., Ganesh Madhan, M.: Numerical analysis on capacity improvement in free space optical link employing two-segment quantum cascade laser-based repeater. Optik **204**, 164216 (2020b)

Ashok, P., Ganesh Madhan, M.: Performance evaluation of free space optical link by incorporating the device parameters of quantum cascade laser-based transmitter. Laser Phys. Lett. **18**, 1–6 (2021a)

Ashok, P., Ganesh Madhan, M.: Impedance characteristics of mid infra-red quantum cascade lasers. J. Opt. Laser Technol. **134**, 106662 (2021b)

Ashok, P., Ganesh Madhan, M., Deepiha, P., Rimmya, C., Piramasubramanian, S.: An efficient chaotic optical signal generation scheme using gain lever effect in bi-section laser diodes. Opt. Commun. **475**, 126202 (2020)

Bai, J., Citrin, D.S.: Design of nonlinearity-enhanced quantum-cascade lasers. Opt. Quant. Electron. **40**, 191–195 (2008). https://doi.org/10.1007/s11082-007-9172-7

Fathololoumi, S., Dupont, E., Chan, C.W.I., Wasilewski, Z.R., Laframboise, S.R., Ban, D., Matyas, A., Jirauschek, C., Hu, Q., Liu, H.C.: Terahertz quantum cascade lasers operating up to 200 K with optimized oscillator strength and improved injection tunneling. Opt. Express **20**, 3866–3876 (2012)

Gopinath, S., Ashok, P., Ganesh Madhan, M.: Performance evaluation of free space optical link driven by gain switched temperature dependent quantum cascade lasers. Laser Phys. Lett. **18**, 1–6 (2021)

Han, M., et al.: Long-wave infrared discrete multitone free-space transmission using a 9.15-μm quantum cascade laser. IEEE Photon. Technol. Lett. **35**(9), 489–492 (2023). https://doi.org/10.1109/LPT.2023.3257843

Hu, Y., Liu, F., Wang, L., et al.: Broad area single mode operation of quantum cascade lasers by integrating porous waveguide and distributed feedback grating. Opt. Quant. Electron. **47**, 515–521 (2015). https://doi.org/10.1007/s11082-014-9886-2

Jirauschek, C., Tzenov, P.: Self-consistent simulations of quantum cascade laser structures for frequency comb generation. Opt. Quant. Electron. **49**, 414 (2017). https://doi.org/10.1007/s11082-017-1253-7

Joharifar, M., et al.: High-speed 9.6-μm long-wave infrared free-space transmission with a directly-modulated QCL and a fully-passive QCD. J. Lightwave Technol. **41**(4), 1087–1094 (2023). https://doi.org/10.1109/JLT.2022.3207010

Kamruzzaman, M.M., Mhatli, S., Arun Kumar, U., et al.: Design of circular photonic crystal fiber for OAM extraction SDM applications. Opt. Quant. Electron. **54**, 864 (2022). https://doi.org/10.1007/s11082-022-04251-0

Kim, D., Curwen, C.A., Wu, Y., Reno, J.L., Addamane, S.J., Williams, B.S.: Wavelength scaling of widely-tunable terahertz quantum-cascade metasurface lasers. IEEE J. Microw. **3**(1), 305–318 (2023). https://doi.org/10.1109/JMW.2022.3224640

Krishna, K., Madhan, M., Ashok, P.: Study of gain switching in vertical cavity surface emitting laser under different electrical pulse inputs. Def. Sci. J. **70**(5), 538–541 (2020)

Kruck, P., Page, H., Sirtori, C., Barbieri, S., Stellmacher, M., Nagle, J.: Improved temperature performance of $Al_{0.33}Ga_{0.67}As$/GaAs quantum-cascade lasers with emission wavelength at $\lambda \approx 11\,\mu m$. Appl. Phys. Lett. **76**, 3340–3342 (2000)

Li, W., et al.: High-power terahertz quantum cascade lasers based on high-Al-composition four quantum wells. IEEE Photon. Technol. Lett. **34**(13), 671–674 (2022). https://doi.org/10.1109/LPT.2022.3181242

Murali Krishna, K., Ganesh Madhan, M., Ashok, P.: Simulation studies on polarization modulated vertical cavity surface emitting laser for combined fiber and free space optical links. Optik **219**, 165018 (2020)

Page, H., Kruck, P., Barbieri, S., Sirtori, C., Stellmacher, M., Nagle, J.: High peak power (1.1 W) (Al) GaAs quantum cascade laser emitting at 9.7 μm. Electron. Lett. **35**, 1848–1849 (1999)
Page, H., Becker, C., Robertson, A., Glastre, G., Ortiz, V., Sirtori, C.: 300 K operation of a GaAs-based quantum-cascade laser at k 9 lm. Appl. Phys. Lett. **78**, 3529–3531 (2001)
Slivken, S., Razeghi, M.: High power, room temperature InP-based quantum cascade laser grown on Si. IEEE J. Quant. Electron. **58**(6), 1–6 (2022). https://doi.org/10.1109/JQE.2022.3212052
Winge, D.O., Wacker, A.: Temperature dependent nonlinear response of quantum cascade structures. Opt. Quant. Electron. **46**, 533–539 (2014). https://doi.org/10.1007/s11082-013-9779-9

Authors and Affiliations

Abdulkarem H. M. Almawgani[1] · B. Ramasubba Reddy[2] · Turki Alsuwian[1] · P. Ashok[3] · C. R. Rathish[4] · M. Ganesh Madhan[5]

✉ P. Ashok
p.ashok@sidtm.edu.in

C. R. Rathish
r.rathish87@gmail.com

[1] Department of Electrical Engineering, College of Engineering, Najran University, Najran, Kingdom of Saudi Arabia

[2] Department of CSE, Anantha Lakshmi Institute of Technology and Sciences, Ànantapur, India

[3] Symbiosis Institute of Digital and Telecom Management (SIDTM), Symbiosis International (Deemed University) (SIU), Lavale, Pune, Maharashtra, India

[4] Department of Computer Engineering, New Horizon College of Engineering, Bengaluru, Karnataka 560103, India

[5] Department of Electronics Engineering, Madras Institute of Technology, Anna University, Chennai, Tamil Nadu, India